The Aachen Shock Tunnel TH2 with Dual Driver Mode Operation

Herbert Olivier

1 Introduction

After more than 50 years, high-enthalpy facilities suitable for aerodynamic testing in the hypersonic regime are still mostly based on the shock tunnel principle. Recent use of these facilities involves the development of space planes, reentry vehicles and scramjets for studying the complex aerothermochemistry associated with these vehicles.

The effects of thermal and chemical relaxation in air become important for flight velocities higher than approximately 3 km/s. In addition, high-enthalpy, aerodynamic-impulse facilities are not only used to study high-temperature effects but are also suitable for generating high Mach number flows at moderate Reynolds numbers to investigate viscosity-dominated effects also at low-enthalpy conditions.

At present, three categories of shock tunnels are in use. The so-called conventional shock tunnel is operated with a driver that is filled up to the desired driver pressure by a preferably light driver gas like helium or hydrogen [1]. In detonation driven shock tunnels [2] the driver section is filled with a detonable gas mixture which is ignited either at the main diaphragm station (backward driver mode) or at the end wall of the driver section (forward driver mode). A detonation wave running through the driver section leaves a highly compressed and heated driver gas behind it. Piston driven shock tunnels employ a nearly adiabatic compression and heating of the driver gas accelerating a heavy piston in the driver towards the main diaphragm station. Especially the last two techniques enable achieving very high shock Mach numbers at reasonably high filling pressures in the driven section, which makes them suitable for aerodynamic high-enthalpy testing. The Aachen shock tunnel TH2 is operated both as conventional and detonation driven shock tunnel.

H. Olivier (✉)
Shock Wave Laboratory, RWTH Aachen University, 52056 Aachen, Germany
e-mail: olivier@swl.rwth-aachen.de

© Springer International Publishing Switzerland 2016

O. Igra and F. Seiler (eds.), *Experimental Methods of Shock Wave Research*,
Shock Wave Science and Technology Reference Library 9,
DOI 10.1007/978-3-319-23745-9_5

2 Operation Principle of the Conventional Shock Tunnel

The elementary shock tube performance is well documented in a number of text books [1, 3–5]. It will thus be sufficient to bring into attention the most important relations and the usual notations of the different flow fields and kind of shock reflections.

A shock tunnel consists of a driver and driven section, a nozzle and a dump tank with a test section. Driver and driven section are separated by the main diaphragm. The driver section is filled with the so-called driver gas, usually helium, at an initial pressure p_4 and a temperature T_4, while the driven section is at an initial pressure p_1 and a temperature T_1 (see Fig. 1). Typical driver pressures are between 10 and 150 MPa and driven gas pressures between 0.01 and 1 MPa. Before the test starts the dump tank is evacuated. Driven section and dump tank are separated by a second thin diaphragm to avoid the inflow of the test gas into the dump tank before the test starts. A double diaphragm technique allows to precisely fill driven and driver sections and to start the shock tunnel run in a controlled manner. Figure 1 shows schematically the setup of the tunnel and the pressure distribution within the shock tube for various times during the run.

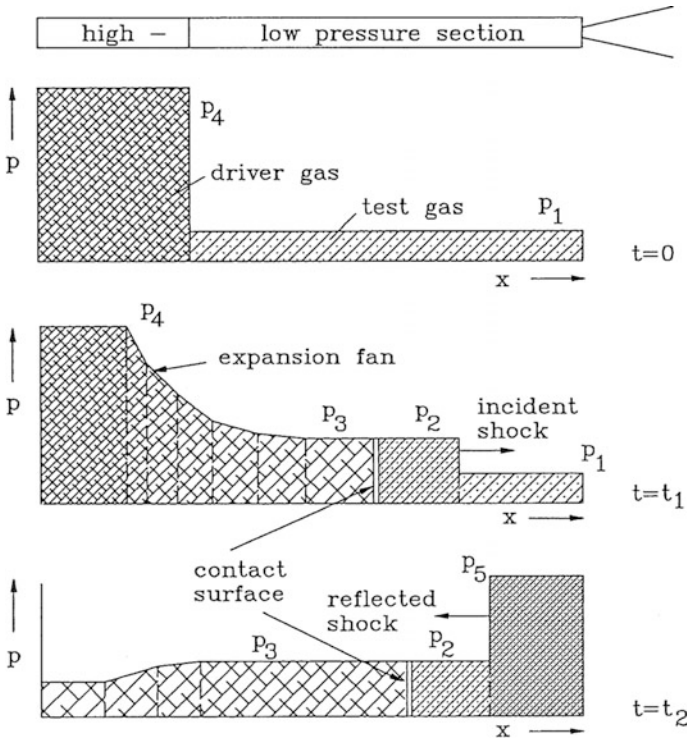

Fig. 1 Schematic setup and operation principle of a conventional shock tunnel

In Fig. 1 ideal diaphragm opening and ideal wave behaviour are assumed (no damping, no boundary layer influence). After rupture of the main diaphragms a primary shock wave propagates into the test gas (1) and compresses it to a pressure p_2 at a temperature T_2 in the region (2). Behind this shock wave a contact surface follows which separates the driver and driven gases. The driver gas acts like a piston which compresses the test gas rapidly. Density and sound velocity on both sides of the interface are different, but pressure and flow velocity are equal in (2) and (3). This pressure balance is produced by an expansion wave the head of which moves upstream into the driver section reducing the pressure continuously from its initial value p_4 to p_2.

A few milliseconds after the bursting of the diaphragm the primary shock wave arrives at the end wall of the driven section. The Aachen shock tunnel operates in the reflected mode, i.e. the primary shock wave is reflected at the end wall due to its relatively small central nozzle inlet and after that propagates upstream (see Fig. 2). During this reflection process the second diaphragm between driven section and nozzle bursts, and the nozzle flow starts. To a first approximation the flow velocity behind the reflected shock is zero if the outflow from the nozzle is neglected. The complete kinetic energy of the shock heated gas in region (2) is thus converted to high values of temperature and pressure in region (5) behind the reflected shock. The compressed test gas having a temperature of a few thousand degrees centigrade subsequently expands through the nozzle. Thus gas of high stagnation enthalpy is converted into a free stream of high velocity in the test section.

After a short time the reflected shock interacts with the contact surface. During this interaction new waves are usually generated which propagate again downstream towards the end wall while the reflected shock moves with changed velocity further upstream (see Fig. 3). In the case of a special combination of the initial gas variables the reflected shock penetrates the contact surface without generating waves of finite amplitudes, the so-called tailored interface case (see Figs. 2 and 3).

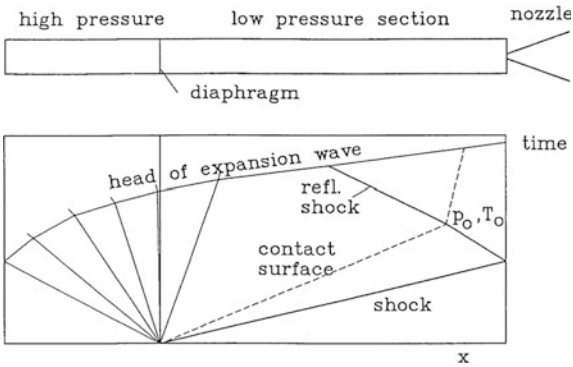

Fig. 2 Wave diagram for tailored interface operation

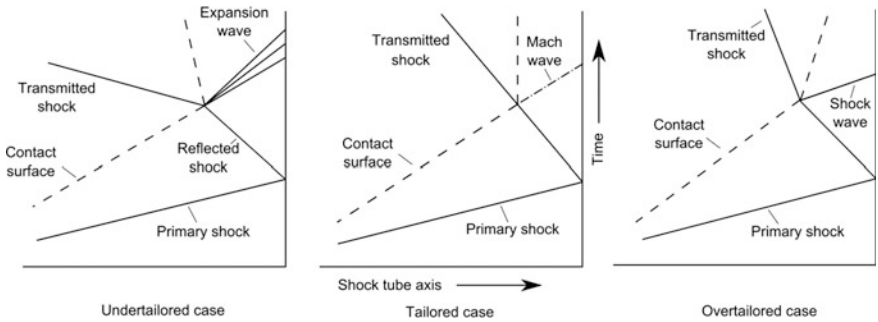

Fig. 3 Interaction of the reflected shock with the contact surface

In the tailored interface case the nozzle reservoir pressure and temperature produced by the initial reflection of incident shock at the end wall persists for a relatively long period.

Figure 3 shows the wave diagram for the tailored and both the under-tailored and over-tailored cases; in the under-tailored case the incident shock wave Mach number is lower than in the tailored case. In this case an expansion wave is generated when the reflected shock and the contact surface interact. In the over-tailored case the incident shock wave Mach number is higher than in the tailored case. This leads to a secondary reflected shock wave and a transmitted shock wave which are generated by the interaction of the initial reflected shock wave with the contact surface.

The secondary reflected shock again reflects at the end wall, and in this way a region of multiple shock reflections develops which leads to an equilibrium nozzle reservoir pressure [6]. The shock tunnel TH2 is generally operated in the tailored and over-tailored interface mode but under-tailored operation is also possible.

The temperature of the test gas behind the reflected shock in the driven section of the shock tube (corresponding to the nozzle "reservoir" or "supply" temperature) is a function of the strength or velocity of the incident shock wave and the initial temperature T_1 of the test gas (air) which is usually equal to the ambient temperature. For given gas combination and initial temperatures of driver and driven gas the shock strength or shock Mach number is a function of the pressure ratio $p_4/p_1 = p_{41}$ across the main diaphragm (see Fig. 4).

Figure 5 shows for various driver/driven gas combinations and for a fixed driver pressure p_4, that for increasing the initial pressure p_1 up to a specific initial pressure (decreasing the shock wave Mach number) the nozzle reservoir pressure p_5 behind the reflected shock wave increases but the temperature T_5 decreases. This generally causes a problem for the binary scaling capabilities of shock tunnels. For simulating the correct dissociation effects behind the bow shock of a re-entry vehicle this scaling law requires for the shock tunnel flow high free stream densities and high flow velocities, i.e. both high nozzle reservoir pressures and temperatures.

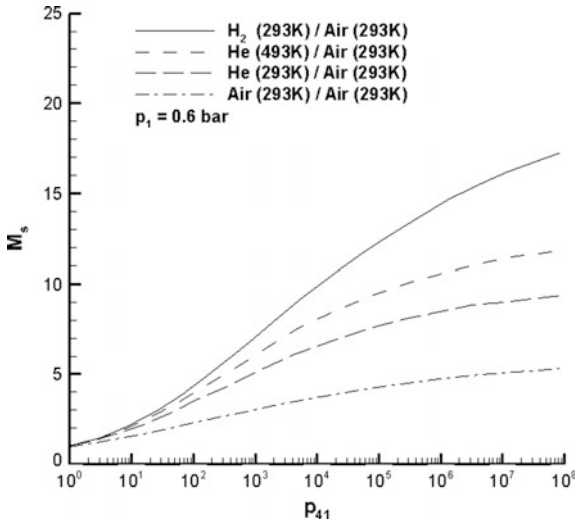

Fig. 4 Shock Mach number M_s as function of pressure ratio p_{41} for different gas combinations; driver gases are assumed as ideal gases, driven gas air as 9 component equilibrium

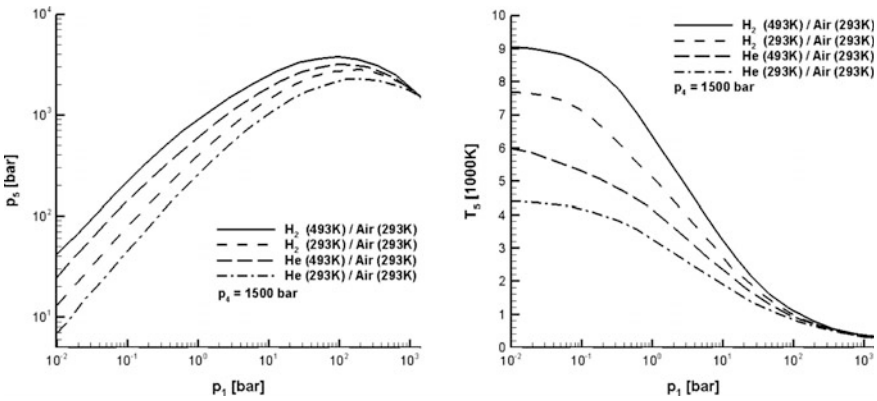

Fig. 5 Influence of the driven gas pressure p_1 on the pressure and temperature behind the reflected shock (p_4 = 1500 bar). Driver and driven gas combinations with their initial temperatures are indicated

3 Setup of the Aachen Shock Tunnel TH2

The shock tube of the Aachen shock tunnel has an inner diameter of 140 mm and a wall thickness of 80 mm. The building which houses the shock tunnel was built especially for the use of such tunnels. A 800 mm steel-enforced concrete wall which separates the driver room from the driven section serves as a protecting wall but is

also used for supporting the recoil absorbing system of the tunnel. There is a sliding joint between the driven section and the nozzle. The nozzle and dump tank compose a single unit which is also connected to the foundation by a recoil damping system. The model support has an independent foundation. Thus even if the receiver or the dump tank may move, the model support is fixed to the laboratory foundation.

3.1 Conventional Helium Driven Shock Tunnel

Driver (length 6 m) and driven section (length 15.4 m) are separated by a double-diaphragm chamber which at maximum pressure utilizes two 10 mm thick stainless steel plates as diaphragms scored in the form of a cross by a milling cutter. Another diaphragm made of brass or copper sheet is located between the driven section and the nozzle entrance. The maximum operating (steady) pressure of the complete tube is 150 MPa. The driver can be electrically heated to a maximum T_4 of 600 K. The exit diameter of the conical nozzle with 5.8° semi-angle amounts to 586 mm. The nozzle throat diameter and therefore the test section flow Mach number can also be changed by inserting different throat pieces. A contoured nozzle with 586 mm exit diameter is available for a nominal exit flow Mach number of 7.

The performance of a shock tunnel expressed as nozzle reservoir pressure and temperature is mainly determined by the Mach number of the incident shock wave and the filling conditions of the driven section. An increase in performance, e.g. in terms of higher stagnation enthalpies requires higher Mach numbers of the incident shock wave. Therefore, a detonation driver has been developed which is in use for more than 15 years.

3.2 Detonation Driven Shock Tunnel

The higher the driver gas pressure and temperature and the lighter the driver gas, the stronger is the incident shock wave for a given filling pressure p_1 in the driven section. The conventional helium driver reaches its operational limits for a driver pressure of about 150 MPa and tube temperatures of about 600 K. To further increase the shock tunnel performance a detonation driver has been developed [7, 8] which alternatively to the helium driver can easily be connected to the driven section.

The detonation driver consists of a 9.4 m long detonation tube and a 6.4 m long damping section which is placed upstream of the detonation section (see Fig. 6). The whole tube has an inner diameter of 140 mm and its maximum working pressure is fixed at 150 MPa. The detonable gas mixture in the detonation section is ignited at the main diaphragm station by an exploding wire. Details about the initiation system and more are given in [8]. After a fast deflagration detonation

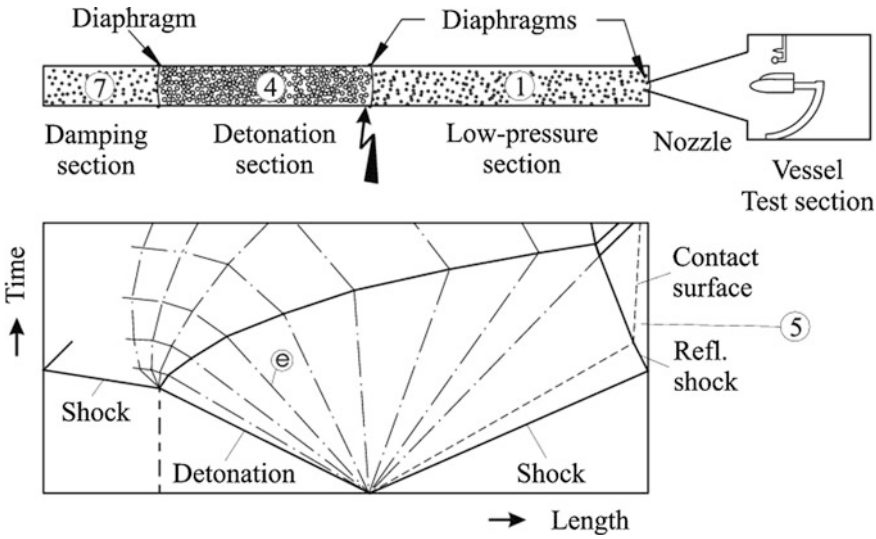

Fig. 6 Principle setup and wave diagram for detonation driven shock tunnel in the upstream mode

transition the detonation wave travels towards the driver section end wall. The damping section is needed for extinguishing the detonation wave before it reflects at the tube end wall. For this, it is filled with nitrogen at relative low pressures. The detonation and damping section are separated by a stack of thin plastic diaphragms which are totally burnt by the detonation wave. The damping section not only reduces the mechanical loading of the tube during the reflection process, it also leads to a longer period of constant driver conditions. In case of no damping section, the detonation wave would reflect as shock wave which propagates towards the main diaphragm station. In case of a damping section, at the location of the diaphragm between detonation and damping section a rarefaction wave develops, the tail of which also travels towards the main diaphragm section. Because the tail of the rarefaction wave travels slower than a reflected shock, in case of a damping section the time of constant flow conditions at the main diaphragm station is longer.

The detonation wave forms as so-called Chapman Jouguet (C-J) detonation which is highly reproducible and stable. This detonation wave is characterized by a high pressure increase across the leading shock front, followed by a Taylor expansion which in case of a closed tube decelerates the flow again to zero velocity. The strength of the detonation wave not only depends on the initial filling pressure but also on the chemical composition of the detonable gas mixture. For the Aachen shock tunnel stoichiometric oxyhydrogen is used with varying admixtures of helium and argon to obtain a wide range of test conditions. Up to a certain limit helium increases the speed of sound of the detonation gas products leading to higher velocities of the detonation wave. Increasing the amount of argon significantly reduces the speed of the detonation wave (see Fig. 7).

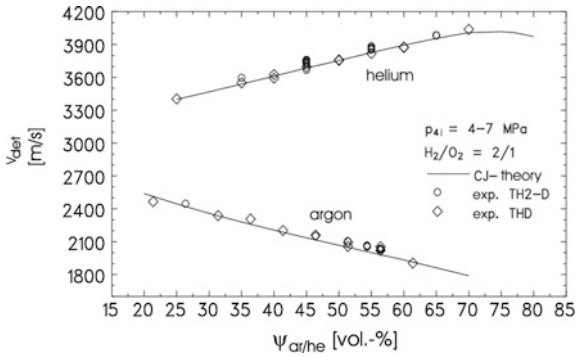

Fig. 7 Influence of helium and argon dilution on the detonation wave velocity for stoichiometric oxyhydrogen mixtures

After rupture of the main diaphragm the incident shock wave propagates along the driven section followed by the driver gas which in case of a detonation driver mainly consists of gaseous water. After the useful running time of the facility this gaseous water would pass through the nozzle leading to strong erosion and water condensation in the test section. To avoid associated problems caused by the gaseous water flow and condensation in the test section, a fast acting valve is in use which originally was developed at the Cornell Aeronautical Laboratory [9]. It works without any external triggering signal or power supply. A sketch of this valve is shown in Fig. 8. When the incident shock wave passes the conical forebody, its overpressure accelerates a piston which via a spring is connected to a plug which after an adjustable time delay closes the nozzle entrance. The central body of the valve is fixed in the shock tube by four thin struts. The operation of this valve is highly reliable and repeatable. The influence of the blockage effect associated with

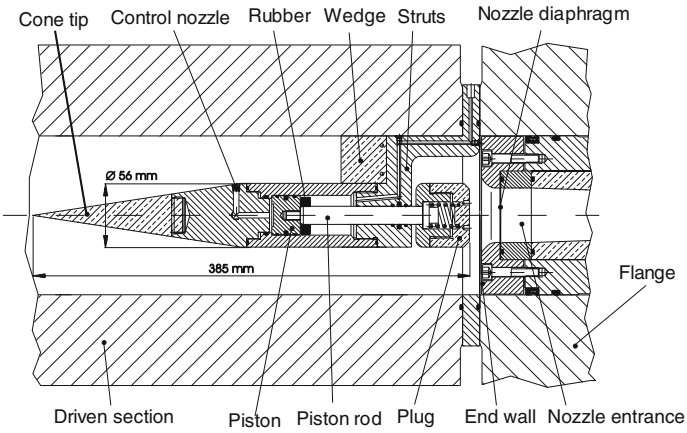

Fig. 8 Fast acting nozzle valve

the nozzle valve has been tested by comparing the reservoir and Pitot pressure histories in experiments conducted with and without a valve. It was found that there is only a very weak influence at the beginning of the run which is not surprising because of the very low flow velocities in front of the shock tunnel nozzle.

3.3 Shock Reflection and Driver Gas Contamination

For reflected shock tunnels a great concern exists concerning premature driver gas contamination of the test gas. There are numerous papers in the literature about this and how to measure or estimate the amount of the driver gas contaminating the test gas.

The mechanism which leads to driver gas contamination is due to bifurcation of the reflected shock at the shock tube wall. Because of the interaction of the reflected shock with the shock tube boundary layer close to the wall, the reflected shock bifurcates into two oblique shocks (see Fig. 9). Using oblique shock wave theory it is straightforward to show that these two shocks do not decelerate the gas to velocity zero as does the straight part of the reflected shock. Therefore, especially after the reflected shock wave has passed the contact surface, a wall jet of cold driver gas forms which penetrates into the region of the shock heated test gas close to the shock tube end wall. This finally leads to a change of the chemical composition of the test gas, but more important to a reduction of the total enthalpy because of the mixing with the cold driver gas. This phenomenon of bifurcation of the reflected shock wave in a shock tube was thoroughly studied by Mark [10] already in the late fifties.

It is obvious that an important criterion determining the total amount of the driver gas penetrating into the test gas is given by the height of the bifurcated shock, i.e. of the triple point. Therefore, the height of the triple point has been determined by flow visualization in a rectangular shock tube which allows the visualization of its entire cross section. In the context of detonation drivers it was of special interest to study this phenomenon for the interaction of the reflected shock with driver gas consisting of gaseous water. As an example, Fig. 10 shows some schlieren pictures

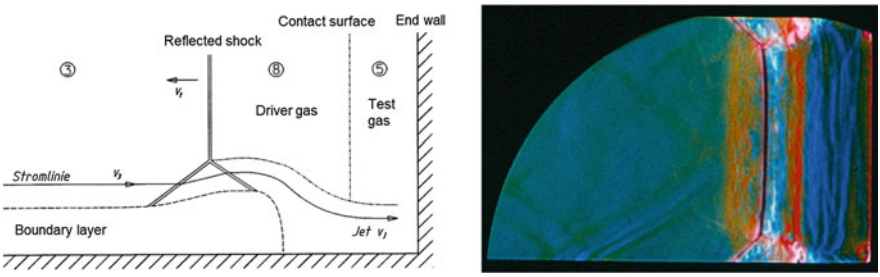

Fig. 9 Sketch of bifurcation of reflected shock

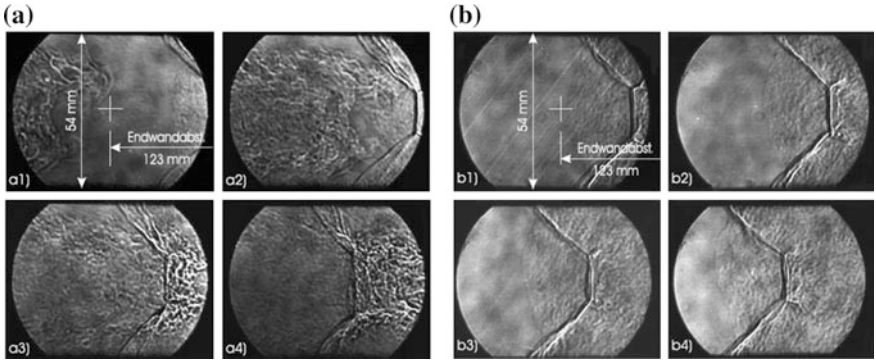

Fig. 10 Interaction of a reflected shock with a contact surface, $Ms = 7.6$, $\Delta t = 12$ μs; **a** helium driver, **b** detonation driver

of the interaction of the reflected shock with a contact surface for the case of a conventional helium driver and a detonation driver. The shock tube end wall is at the right side of the picture and the contact surface becomes visible, especially in the first picture in case of the helium driver. As expected, it is not a planar surface but wrinkled and showing a strong shock tube boundary layer influence. In the case of the detonation driver no contact surface could be visualized, the reason for which is the small density difference between the shock heated test gas and the still relatively hot driver gas.

Nevertheless, calculations of the shock tube flow prove that for the visualized region in front of the shock tube end wall as in the case of the helium driver the interaction with the contact surface takes place. Due to strength limitations of the windows and the shock tube, the initial pressure p_1 for these experiments was limited to 0.4 kPa which resulted in a thick shock tube boundary layer and therewith in a large shock bifurcation. However, the comparison between the results for the helium and detonation driver allows a first statement whether the detonation driver leads to a stronger shock bifurcation or not. From these figures the height of the bifurcated shock has been measured and plotted versus the distance from the end wall (see Fig. 11). For the detonation driver two results are given, one for a stoichiometric hydrogen/oxygen mixture diluted with helium and one for argon as additive. Close to the end wall and for distances more than 120 mm from the end wall the heights of the triple points are identical for the conventional helium driver and the detonation driver. Only in the region at about x = 120 mm does the height decrease for the helium driver, but further away from the end wall it approaches the value for the detonation driver.

From these experiments it can be expected that there is no significantly different behaviour in shock bifurcation for the two types of drivers. Therefore it might be expected that also the magnitude of driver gas contamination is similar for both cases which is confirmed by free stream measurements.

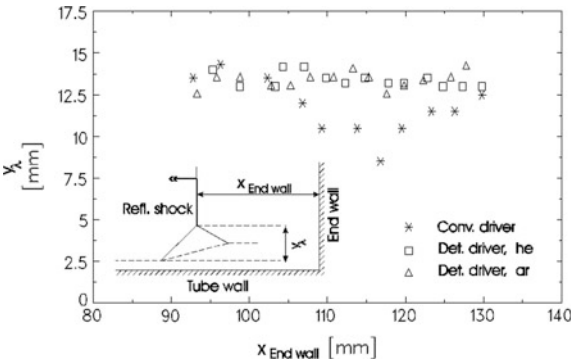

Fig. 11 Height of triple point of reflected shock for helium and detonation driver

The developing shock tube boundary layer behind the incident shock leads to a continuous reduction of its speed and therewith of its strength. This shock attenuation should be proportional to the boundary layer thickness and the flow Mach number behind the incident shock. Of course, the tube diameter has an inverse influence. The attenuation of the shock speed has been measured for a variety of test conditions close to the end wall of the shock tube. It turns out that for the shock tunnel TH2 with 140 mm inner diameter the shock attenuation is nearly constant and in the average amounts to 1.2 % per meter [8]. This shock attenuation as well as losses caused by the diaphragm opening and other dissipative mechanisms lead to a loss of performance of the shock tube compared to an ideal shock tube process. The losses can easily be determined by comparing the computed pressure and enthalpy behind the reflected shock based on the measured shock speed with the values for an ideal inviscid, adiabatic shock tube process. As for the shock attenuation, the total pressure and enthalpy losses are almost independent of the considered shock tube conditions with respect to the ideal values. For both, the helium and detonation driven mode the relative losses of the nozzle reservoir pressure and total enthalpy amount to 30 %. This is a quite realistic value for shock tunnels of this size and has to be taken into account when choosing driver gas conditions.

3.4 Nozzle Reservoir and Free Stream Flow Conditions

A conical nozzle with 5.8° half opening angle and 586 mm nozzle exit diameter accelerates the shock-compressed, heated gas to hypersonic velocities in the test section. Behind the nozzle exit a permanent Pitot and static pressure probe, as well as a small sphere for measuring the stagnation point heat flux are installed. From these signals the time-resolved free stream conditions, especially u_∞ and ρ_∞ are resolved employing a suitable data reduction technique which is based on applicable gas dynamic relations [11].

As examples, Figs. 12 and 13 show the time histories of the nozzle reservoir pressure p_0, the Pitot pressure p_{t2}, the free stream static pressure p_∞ and of the

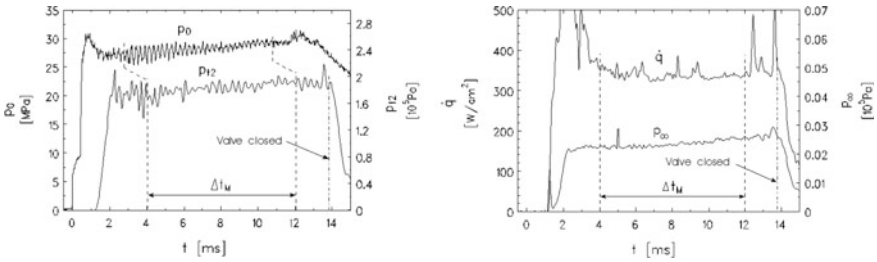

Fig. 12 Reservoir (p_0) and test section conditions (p_{t2}, $\dot{q}$, p_∞) for h_0 = 2.4 MJ/kg total enthalpy

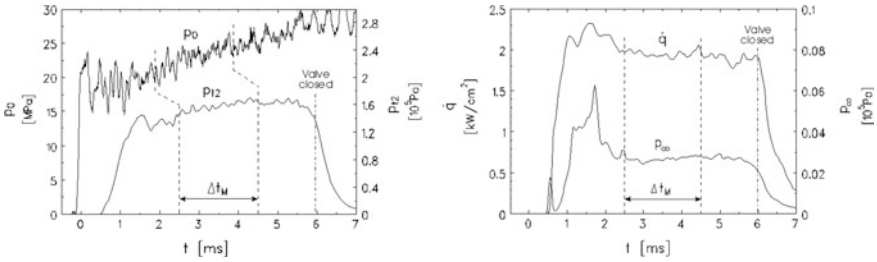

Fig. 13 Reservoir (p_0) and test section conditions (p_{t2}, $\dot{q}$, p_∞) for h_0 = 14.4 MJ/kg total enthalpy

stagnation point heat flux $\dot{q}$ measured at a small sphere of 20 mm diameter in the test section. These measurements have been performed in the detonation driven mode for a relatively low enthalpy and for the maximum one of 14.4 MJ/kg at which the detonation driver is used so far.

For the low enthalpy case a useful testing time of about 8–10 ms can be identified, whereas for the high-enthalpy case it reduces to 2 ms. After 14 and 6 ms, respectively, the fast acting valve closes the nozzle entrance which causes the rapid drop of the flow parameter in the test section. The high-enthalpy condition is slightly over-tailored which causes the weak pressure rise in the nozzle reservoir.

The free stream has been calibrated by Pitot rake measurements at various positions downstream of the nozzle exit. The Pitot rake was equipped with a total of 38 small spheres, each instrumented with a combined coaxial thermocouple allowing a heat flux and Pitot pressure measurement at the stagnation point of the sphere. Additionally, a free stream static pressure probe was installed on the rake. From this data, the Pitot pressures as well as the total temperature profiles have been deduced, employing for the latter one the formula of Fay and Riddell (Figs. 14 and 15). The Pitot pressure profiles show a typical core flow region of constant pressure and a drop across the nozzle boundary layer, i.e. in the free shear layer downstream of the nozzle exit. For the most upstream position, i.e. 20 mm downstream of the nozzle exit, the dashed line in the Pitot pressure profile indicates the boundary layer thickness according to the Edenfield correlation [12] for nozzle flows. The agreement with the measured thickness is very good which holds for both the low- and

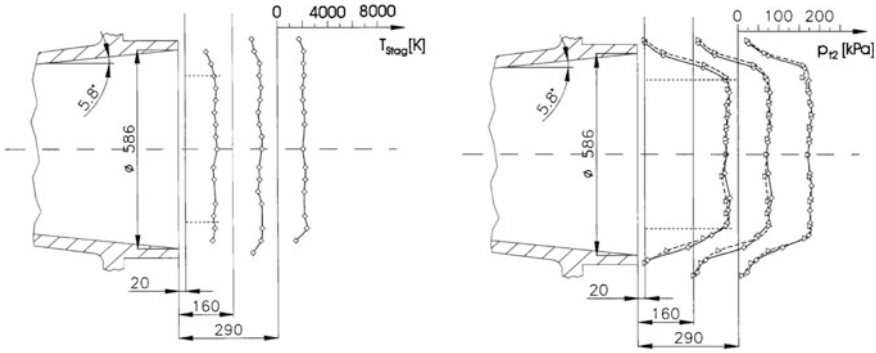

Fig. 14 Pitot pressure and total temperature profiles for three axial positions downstream of the nozzle exit, h_0 = 2.4 MJ/kg

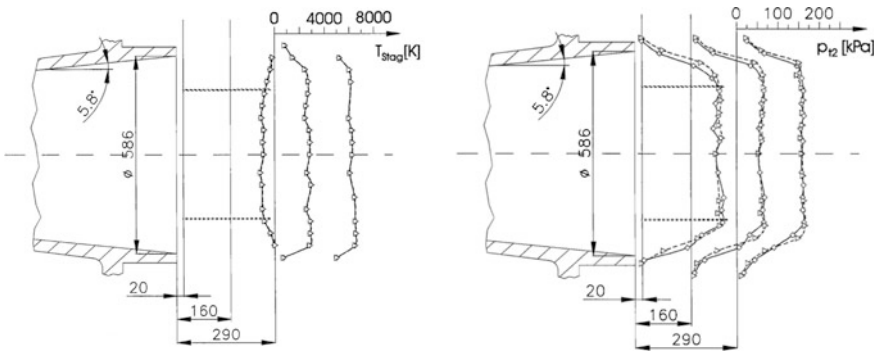

Fig. 15 Pitot pressure and total temperature profiles for three axial positions downstream of the nozzle exit, h_0 = 14.4 MJ/kg

high-enthalpy flow. Within the free shear layer the deduced total temperatures are questionable because the Mach number drops significantly and the validity of Fay and Riddell's formula is violated.

As known, the conical nozzle leads to axial flow gradients which become apparent by a decrease of the Pitot and free stream static pressure in downstream direction. For the considered nozzle this results in a Mach number increase of 4.2 % along a distance of 300 mm. This is of some disadvantage compared to contoured nozzles and has to be taken into account for long model geometries or the investigation of Mach number sensitive phenomena. However, a conical nozzle easily allows varying the free stream Mach number and thereby other flow parameters by changing the throat diameter. Furthermore, the shape of conical nozzles does not lead to a focusing of pressure disturbances towards the nozzle axis, as it happens for contoured nozzles.

Table 1 Typical flow conditions of the shock tunnel TH2

Reservoir conditions			Nozzle exit values			
p_0 (MPa)	T_0 (K)	h_0 (MJ/kg)	u_∞ (m/s)	ρ_∞ (kg/m^3)	M_∞	Re_∞ (10^6/m)
7.0	1520	1.7	1745	2.1×10^{-2}	7.7	4.1
17.5	2500	3.0	2350	2.7×10^{-2}	7.4	4.0
32.5	3640	4.1	2910	3.2×10^{-2}	6.8	3.7
56.0	4600	6.5	3400	3.6×10^{-2}	6.5	3.7
26.5	5520	9.0	3950	1.3×10^{-2}	5.8	1.3
22.0	7400	14.4	4850	0.76	5.3	0.8

The shock tunnel TH2 is operated for low as well as medium to high total enthalpies ranging from 1.7 to 14.4 MJ/kg. Up to 6.5 MJ/kg the conventional helium driver is used which in this case is filled with helium at 120 MPa and the whole driver is electrically heated to 570 K. The detonation driver is capable of generating low as well as high total enthalpies, but which is usually operated only for high-enthalpy conditions. Some typical test conditions covering the whole simulation range are listed in Table 1. The free stream conditions are given at the nozzle exit for the conical nozzle with 5.8° half opening angle.

The Mach numbers given in Table 1 have been determined under the assumption of an equilibrium nozzle flow which is not totally correct, especially for the flow conditions at the two highest total enthalpies. The free stream conditions have been derived from the measured Pitot pressure and stagnation point heat flux employing the method described in [11]. Therefore deviations may occur from those values based on a nozzle flow calculation.

3.5 Driver Gas Detection by the Free Stream Static Pressure

Reliable measurements in reflected shock tunnels require a detailed knowledge of the amount of driver gas contamination of the test gas. The mechanism leading to driver gas contamination is due to bifurcation of the reflected shock as described above. The useful testing time of shock tunnels should not be defined by the time period of constant reservoir or Pitot pressure. Even the measured time history, for example, of the stagnation point heat flux in the free stream might not be adequate to determine a useful testing time window because parameters like the heat flux, Pitot pressure etc. mainly depend on the free stream density and velocity. A contamination of the test gas by cold driver gas leads to a decrease of the free stream velocity caused by a reduced total temperature. On the other hand the reduced temperature leads to higher densities so that flow parameters like Pitot pressure, stagnation point and heat flux might not be strongly influenced by driver gas contamination. This effect is visible in the experimental data of reflected shock tunnels. The mixing of the hot test gas with the cold driver gas leads not only to

lower total temperatures but also to a change of the isentropic exponent. For example, in case of helium as driver gas the isentropic exponent increases. This partially offsets the effect of the reduced total temperature on the free stream density and velocity.

However, the equations of quasi-onedimensional, isentropic flow show that for a fixed nozzle area ratio and nozzle reservoir pressure an increase of the isentropic exponent leads to higher flow Mach numbers and therewith to lower free stream static pressures. The proposed method of driver gas detection by the free stream static pressure measurement is based on this effect. In literature other methods are described as well. Paull developed a sensor for driver gas detection in which with increasing driver gas amount an oblique shock steepens up and finally blocks a channel flow [13]. The time of the blockage indicates a certain level of driver gas contamination. This sensor has been modified and used in the T5 shock tunnel by Sudani and Hornung [14]. Mass spectrometry to determine the arrival time of helium in the test gas has also been used [15] but this is much more complicated compared to sensor based methods.

Experiments have been performed with the conventional helium driver measuring the free stream static pressure with a small static pressure probe [16]. Figure 16 shows the histories of the nozzle reservoir pressure p_0, of the Pitot pressure p_{t2} and of the free stream static pressure p_∞ for an over-tailored test condition. Whereas the Pitot pressure nicely follows the temporal behaviour of the reservoir pressure, the free stream static pressure shows a substantial decrease after its initial rise. For tailored-interface conditions the free stream static pressure signal follows the Pitot pressure as expected. This static pressure drop is caused by driver gas contamination leading to a temporal rise of the isentropic exponent. The mixture of air ($\gamma = 1.4$) and helium ($\gamma = 1.66$) results in an increase in γ of the test gas. For a nozzle with constant area ratio A/A^* (A^* is the throat area), an increase of

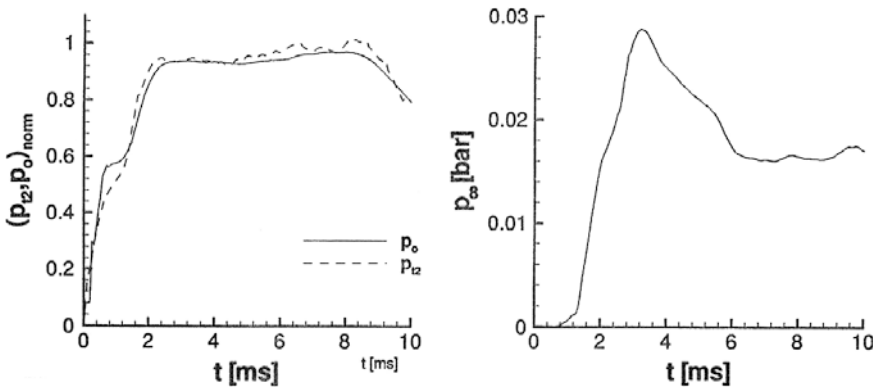

Fig. 16 Nozzle reservoir (p_0), Pitot (p_{t2}) and free stream static pressure (p_∞) histories for strongly over-tailored test conditions

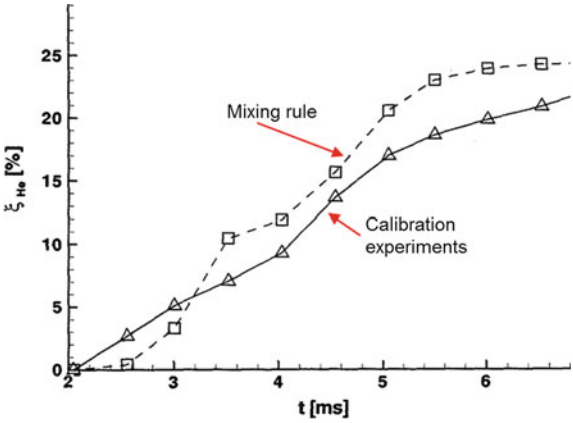

Fig. 17 Temporal increase of helium concentration in the test gas for over-tailored test condition

the isentropic exponent leads to a higher Mach number and therewith to a lower free stream static pressure for a given reservoir pressure.

The amount of the helium contamination can be derived from the measured static and total pressure. Based on ideal gas relations, this pressure ratio p_∞/p_0 can be expressed as a function of the nozzle area ratio and of the isentropic exponent γ which allows determining the actual isentropic exponent as a function of time. The appropriate γ is given by the mixing rule for air and helium:

$$\gamma = \frac{\xi_{air} \cdot c_{p,air} + \xi_{He} \cdot c_{p,He}}{\xi_{air} \cdot c_{v,air} + \xi_{He} \cdot c_{v,He}} \tag{1}$$

which allows to find the helium mass fraction. This procedure has been applied for the broken curve in Fig. 17 which gives the deduced helium mass fraction for the pressure traces shown in Fig. 16. For high-enthalpy conditions this method would be cumbersome, because in this case no simple relation is available between the pressure ratio p_∞/p_0 and the isentropic exponent.

Numerical simulations of the nonequilibrium nozzle flow or other methods would be necessary to determine this relation. However, this extensive method and its uncertainties due to the numerical simulation can be avoided by a calibration procedure. In this case, the relation between the free stream static pressure and the driver gas contamination is experimentally determined.

The low pressure section of the shock tube is filled with a known mixture of helium and air. Then, for the considered reservoir conditions and preferably for tailored interface operation the free stream static pressure is measured in the test section. Figure 18 shows typical time histories of the static pressure for various helium concentrations, normalized with the Pitot pressure.

From Fig. 18 it is obvious that with increasing helium mass fraction the ratio p_∞/p_{t2} decreases. This data can be used as calibration data to obtain the level of helium concentration from the measured static and Pitot pressure. This procedure has been applied for the dashed line in Fig. 17. The agreement between the two

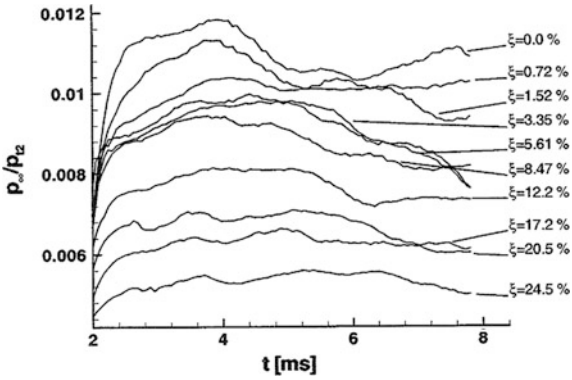

Fig. 18 Time histories of the pressure ratio p_∞/p_{t2} for various helium concentrations

methods is reasonably good and the accuracy achieved is comparable to that of other methods. After the useful testing time of about 4 ms the helium concentration amounts to about 20 % which is also comparable to values given in the literature (see e.g. [14]).

For pure air as the test gas or for a very low helium concentration the pressure ratio history in Fig. 18 should show a more or less flat or constant behaviour as for the higher helium concentrations. But after 4 ms for the very low helium concentrations a decrease of the pressure ratio occurs which indicates that even for this nominal tailored-interface condition the interaction of the reflected shock with the contact surface causes an additional driver gas contamination. This results in a higher helium concentration than the chosen nominal premixed one. Therefore in this case the pressure ratio has been determined from the measured signals just after flow establishment where the additional driver gas contamination due to the reflected shock is still negligible.

The advantage of the described method of driver gas detection based on free stream static pressure measurements is that it does not need any additional measuring device except a permanently installed free stream static pressure probe in the test section. Therefore it can be run in parallel to any other measurements or wind tunnel model testing.

4 Summary

Shock tunnels working in the reflected mode are in worldwide use for studying hypersonic flows from the low- to the high-enthalpy regime. They mainly differ in their driver principle which comprises the classical driver utilizing pre-compressed gas, combustion and detonation driver and the free piston driver. With the largest existing shock tunnels, the detonation driven facility JF12 in China and the free piston driven shock tunnel HIEST in Japan, today's available technology seems to be at an upper limit because of material problems and substantial operational requirements.

The working principle of shock tunnels leads to the reality that the higher the total enthalpy the shorter the measuring time. Other side effects have to be considered for data assessment.

Overall, nonequilibrium nozzle flow at high-enthalpy conditions, driver gas contamination, time varying flow conditions and short running times have different influences on the quality of the results. Some aspects of shock tunnel operation are reasonably well understood, others like specific shock tunnel effects on boundary layer transition for example are far from being understood.

Nevertheless, at present only shock tunnels offer the possibility of performing aerodynamic tests of sufficient quality at high-enthalpy conditions with wind tunnel models large enough to house an extensive instrumentation. In recent years not only the external flow around vehicles has been considered, but even the internal flow in large scramjet models including injection and combustion of different types of fuel has been successfully examined. For studying wall temperature sensitive flow phenomena the drawback of shock tunnels of low model wall temperatures can be avoided, or at least reduced, by heating the model wall up to the desired temperature prior to the experiment.

In summary, shock tunnels are a powerful tool for studying high-enthalpy, hypersonic flows in ground based facilities. As has been proven, careful operation and data reduction methods result in reliable data with acceptable uncertainty margins.

References

1. Hertzberg, A., Witliff, C.E., Hall, J.G.: Summary of Shock Tunnel Development and Application in Hypersonic Research. AFOSR TR 60–139. Cornell Aeronautical Laboratories, New York (1961)
2. Yu, H.R., Esser, B., Lenartz, M., Groenig, H.: Gaseous detonation driver for a shock tunnel. Shock Waves **2**(4), 245–254 (1992)
3. Thompson, P.: Compressible Fluid Dynamics. McGraw-Hill Book Company, New York (1972)
4. Liepmann, H.W., Roshko, A.: Elements of Gasdynamics. Wiley, New York (1960)
5. Glass, I.I., Sislian, J.P.: Nonstationary Flows and Shock Waves. Oxford University Press, Oxford (1994)
6. Copper, J.A.: Experimental investigation of the equilibrium interface technique. Phys. Fluids **5**, 844–849 (1962)
7. Yu, H.R.: Oxyhydrogen combustion and detonation driven shock tube. Acta. Mech. Sin. **5**(2), 97–107 (1999)
8. Olivier, H., Zonglin, J., Yu, H.R., Lu, F.K.: Detonation-driven shock tubes and tunnels. In: Lu, F., Marren, D. (eds.) Advanced Hypersonic Test Facilities. Progress in Astronautics and Aeronautics, vol. 198, pp. 135–203. AIAA Inc, USA (2002)
9. Bird, K.D., Martin, J.F., Bell, T.J.: Recent developments in the use of the hypersonic shock tunnel as a research and development facility. In: Proceedings 3rd Hypervelocity Techniques Symposium, Denver, USA (1964)
10. Mark, H.: The Interaction of a Reflected Shock Wave with the Boundary Layer in a Shock Tube. NACA TM 1418, (1958)

11. Olivier, H.: An improved method to determine free stream conditions in hypersonic facilities. Shock Waves **3**, 129–139 (1993)
12. Edenfield, E.E.: Contoured Nozzle Design and Evaluation for Hotshot Tunnels, pp. 68–369. AIAA, USA (1968)
13. Paull, A.: A simple shock-tunnel driver gas detector. In: Sturtevant, B., Shepherd, J.E., Hornung, H.G. (eds.) Proceedings 20th International Symposium on Shock Waves, pp. 1557–1562, Pasadena, USA (1995)
14. Sudani, N., Hornung, H.G.: Detection and reduction of driver gas contamination in a high-enthalpy shock-tunnel. In: Boyce, R.R. et al. (eds.) Proceedings 21st International Symposium on Shock Waves, pp. 543–548, Great Keppel Island, Australia (1997)
15. Skinner, K.A.: Mass spectrometry in shock tunnel experiments of hypersonic combustion. Ph.D thesis, University of Queensland, Australia (1994)
16. Kindl, H., Olivier, H., Zhao, H., Muylaert, J., Wong, H., Walpot, L.: Conventional flow diagnostics in shock tunnels. In: Boyce, R.R. et al. (eds.) Proceedings 21st International Symposium on Shock Waves, pp. 493–498, Great Keppel Island, Australia (1997)

Author Biography

Herbert Olivier is working on high speed flows and shock tube technology at the Shock Wave Laboratory of RWTH Aachen University. His research activities cover trans-, super- and hypersonic flows, ignition phenomena of fuels, and various topics of interdisciplinary applications of shock waves for industrial use. As editor of the Shock Waves Journal and reviewer of most important international journals he is involved in the reviewing process of scientific papers related to various fields of fluid and gas dynamics. He is member of the International Advisory Committee of the Shock Wave Symposium and of other international organizations. He received his Diploma degree in aeronautics from RWTH Aachen University in Germany and his 'Dr.-Ing'. degree from the same university. Since 1996 he is head of the Shock Wave Laboratory at RWTH Aachen University. Current interests among others are related to film cooling and Görtler vortices in super- and hypersonic flows, unsteady transonic airfoil flow, ignition phenomena in hydro-carbon fuels, development of fast thermocouples.